MIT Open Access Articles

The transcription factor BATF operates as an essential differentiation checkpoint in early effector CD8[superscript +] T cells

The transcription factor BATF operates as an essential differentiation checkpoint in early effector CD8+ T cells

Makoto Kurachi[1,2,*], **R. Anthony Barnitz**[3,*], **Nir Yosef**[5], **Pamela M. Odorizzi**[1,2], **Michael A. Dilorio**[3], **Madeleine E. Lemieux**[6], **Kathleen Yates**[3], **Jernej Godec**[3], **Martin G. Klatt**[3], **Aviv Regev**[5,7], **E. John Wherry**[1,2,#], and **W. Nicholas Haining**[3,4,5,#]

[1]Department of Microbiology University of Pennsylvania Perelman School Medicine, Philadelphia, PA, USA

[2]Institute for Immunology, University of Pennsylvania Perelman School Medicine, Philadelphia, PA, USA

[3]Department of Pediatric Oncology, Dana-Farber Cancer Institute Children's Hospital, Harvard Medical School, Boston, MA, USA

[4]Division of Hematology/Oncology, Children's Hospital, Harvard Medical School, Boston, MA, USA

[5]Broad Institute of MIT and Harvard, 7 Cambridge Center, Cambridge, MA, USA

[6]Bioinfo, Plantagenet, Ontario, Canada

[7]Howard Hughes Medical Institute, Department of Biology, Massachusetts Institute of Technology, Cambridge, MA, USA

Abstract

The transcription factor BATF is required for interleukin 17 (IL-17)-producing helper T cell (T$_H$17) and follicular helper T cell (T$_{FH}$) differentiation. Here, we show that BATF also has a fundamental role in regulating effector CD8$^+$ T cell differentiation. BATF-deficient CD8$^+$ T cells show profound defects in effector expansion and undergo proliferative and metabolic catastrophe early after antigen encounter. BATF, together with IRF4 and Jun proteins, binds to and promotes early expression of genes encoding lineage-specific transcription-factors (T-bet and Blimp-1) and cytokine receptors, while paradoxically repressing genes encoding effector molecules (IFN-γ and granzyme B). Thus, BATF amplifies TCR-dependent transcription factor expression and augments

inflammatory signal propagation but restrains effector gene expression. This checkpoint prevents irreversible commitment to an effector fate until a critical threshold of downstream transcriptional activity has been achieved.

Upon activation by antigen, costimulation and inflammation, naive CD8^{+} T cells initiate a program of clonal expansion and differentiation resulting in wide-spread changes in expression of genes involved in cell-cycle, metabolism, effector function, apoptosis, and homing[1, 2, 3, 4]. This large-scale transcriptional reprogramming results in irreversible and heritable alterations in the function of the cell and in the fate of its progeny.

Several transcription factors (TFs) including T-bet, Eomes, Runx3, Id2 and Blimp-1 are known to regulate the expression of genes essential for CD8^{+} effector T cells such as IFN-γ and perforin[5, 6, 7]. However, CD8^{+} T cells that lack T-bet, Eomes, Id2 or Blimp-1 acquire many features of normal effector T cells and are competent to form T cell memory[8, 9, 10, 11, 12, 13]. One interpretation of these relatively mild defects in single transcription factor (TF)-deficient settings is that functional redundancy exists between TFs known to be involved in CD8^{+} effector differentiation. Alternatively, or in addition, other TFs may exist that are upstream and/or more fundamental to the regulation of CD8^{+} T cell differentiation.

Basic leucine zipper transcription factor ATF-like (BATF) is a bZIP transcription factor that plays an important role in regulating differentiation and function in many lymphocyte lineages[14, 15, 16, 17, 18]. In the CD8^{+} T cell lineage, increased expression of BATF in exhausted CD8^{+} T cells suppresses their effector function[19]. In the CD4^{+} T cell lineage, BATF is required for the differentiation of interleukin 17 (IL-17)-producing helper T cells (T$_H$17)[14], where it binds co-operatively with the transcription factor IRF4[20, 21, 22] and its dimerization partners c-Jun, JunB and JunD[18]. BATF is also important for the development of follicular helper T cells (T$_{FH}$) by regulating the transcription factors Bcl-6 and c-Maf[15, 16]. In addition, BATF is required for class-switch recombination in B cells and to regulate activation-induced cytidine deaminase[16] as well as DNA damage checkpoint in hematopoietic stem cell (HSC) self-renewal[23]. Chromatin immunoprecipitation and high-throughput sequencing (ChIP-Seq) studies in T$_H$17 cells suggest that BATF may play a critical role in regulating the expression of many lineage-specific genes in concert with other TFs, possibly by functioning as a 'pioneer factor' that nucleates transcriptional complexes at key regulatory regions[22]. The role of BATF in effector CD8^{+} T cell differentiation, in contrast, is not fully understood.

Here, we show that BATF is a central regulator of early effector CD8^{+} T cell differentiation. CD8^{+} T cells that lack BATF have a profound inability to undergo normal naive to effector differentiation and proliferative expansion. ChIP-Seq and transcriptional profiling studies showed that BATF bound to and/or promoted expression of key transcriptional regulators of effector differentiation (T-bet, Blimp-1, Runx3), cytokine receptors and their signal transducers (e.g. IFNAR, IL-12R, IL-2R, STATs). However, BATF also repressed many of the genes encoding effector molecules downstream of these transcription factors and cytokine signaling pathways (IFN-γ and granzyme B). The absence of BATF resulted in a near complete collapse in effector CD8^{+} T cell differentiation shortly after activation and

this collapse was associated with major defects in cellular metabolism, proliferation, and survival pathways. The dual role of BATF in upregulating effector transcription factors while restraining effector molecule expression may provide a regulatory circuit that sets the threshold for commitment to an effector CD8^{+} T cell fate.

Results

BATF is required for CD8^{+} T cell effector differentiation

BATF expression is upregulated in effector CD8^{+} T cells responding to lymphocytic choriomeningitis virus (LCMV) infection and remains elevated in memory CD8^{+} T cells compared to naive CD8^{+} T cells [19]. We therefore asked whether BATF played a role in regulating the CD8^{+} T cell response *in vivo*. We infected BATF knockout (*Batf*^{−/−}), BATF heterozygous (*Batf*^{+/−}), and wild-type mice with the Armstrong (Arm) strain of LCMV that initiates an acute infection and tracked the resulting CD8^{+} T cell response to the LCMV gp33 epitope using tetramers. We found significantly fewer LCMV Db gp33-specific CD8^{+} T cells in *Batf*^{−/−} mice compared with *Batf*^{+/−} or wild-type mice (Fig. 1a and b) at th e peak of the effector response (day 8 post-infection [d8 p.i.], **$P<0.01$) as well as at later time points (d15, d22 and d40 p.i.). This finding was not due to altered distribution as we found a similar decrease in cell numbers in the spleen and other organs (Fig. 1c and data not shown). The phenotype of naive CD8^{+} T cells in *Baft*^{−/−} mice appeared similar to wild-type cells (data not shown), and thymic development has been reported to be unperturbed in the absence of *Batf*[14]. These results suggested a defect in the activation and differentiation of effector CD8^{+} T cells without BATF.

Batf^{−/−} effector CD8^{+} T cells displayed a CD27^{lo}CXCR3^{lo}KLRG1^{hi}CD127^{lo} phenotype (Supplementary Fig. 1a), and sustained higher granzyme B protein expression in the memory phase (Supplementary Fig. 1b), which taken together is consistent with a more activated and/or terminally differentiated phenotype[3, 7]. However, protein expression of both T-bet and Eomes was decreased in *Batf*^{−/−} CD8^{+} T cells (Supplementary Fig. 1c), suggesting that the increase in KLRG1^{+} effector or memory *Batf*^{−/−} CD8^{+} T cells was not simply due to a sustained increase in T-bet and/or Eomes[10]. The defect in effector T cell generation following LCMV infection was not limited to CD8^{+} T cells. We found that the virus-specific CD4^{+} T cell response was also severely diminished in *Batf*^{−/−} animals (Supplementary Fig.1d-g). These defects in primary T cell responses resulted in a major defect in viral control as mice lacking BATF failed to contain LCMV Arm replication *in vivo* (Fig. 1d). Thus, loss of BATF resulted in severely defective effector CD8^{+} and CD4^{+} T cell clonal proliferation and altered effector differentiation.

BATF is required in a CD8^{+} T cell-intrinsic fashion

BATF is involved in multiple immune cell lineages[17] and it is unclear whether the effector CD8^{+} T cell defects described above were due to an intrinsic role of BATF or secondary effects of failed viral control. To directly test whether the requirement for BATF in effector CD8^{+} T cell differentiation was cell intrinsic, congenically distinct *Batf*^{−/−} and wild-type P14 CD8^{+} T cells (specific for the LCMV gp33 epitope presented on H-2Db) were adoptively transferred at 1:1 ratio into naive wild-type recipients. One day later, the mice

were infected with LCMV Arm. The naive $Batf^{-/-}$ and wild-type P14 CD8$^+$ cells were phenotypically similar at transfer (Supplementary Fig. 2a). However, by d8 p.i., the number of $Batf^{-/-}$ P14 effector CD8$^+$ T cells was profoundly decreased (up to 400 fold) compared with wild-type P14 cells (Fig. 2a). The ratio of $Batf^{-/-}$ to wild-type P14 cells was relatively stable following the effector phase (d8 p.i.) through long-term memory (d200+ p.i.), suggesting that the critical requirement for BATF was in initial effector differentiation and clonal proliferation (Fig. 2b). We excluded rejection of $Batf^{-/-}$ CD8$^+$ T cells as a cause for the cell loss by transferring $Batf^{-/-}$ and wild-type P14 cells into lympho-replete hosts in the absence of infection and found equivalent persistence of both types of cells over 40 days (Supplementary Fig. 2b). The decrease in $Batf^{-/-}$ P14 effector CD8$^+$ T cell clonal proliferation was not a result of competition with wild-type P14 cells or skewed tissue distribution because individual adoptive transfer of wild-type versus $Batf^{-/-}$ P14 cells into separate recipient mice gave similar results, and the reduced frequency of $Batf^{-/-}$ P14 cells was consistent in multiple lymphoid and non-lymphoid organs at both the effector and memory phase (Supplementary Fig. 3a-c). In addition, the response of $Batf^{+/-}$ P14 cells was nearly identical to wild-type P14 cells, suggesting that sufficient expression of BATF for an optimal CD8$^+$ T cell response can be achieved in the absence of one allele of $Batf$ (Supplementary Fig. 3a and b).

We observed a similar defect in effector CD8$^+$ T cell differentiation for $Batf^{-/-}$ P14 cells in $Listeria\ monocytogenes$ infection or immunization with peptide-pulsed dendritic cells (Supplementary Fig. 4), indicating that the requirement for BATF in effector CD8$^+$ T cell differentiation is not limited to LCMV infection. The difference in $Batf^{-/-}$ P14 cell responses between LCMV versus LM infection or DC immunization may be due to the greater signal strength and/or antigen dose during LCMV infection, consistent with recent observations on the role of IRF4 in regulating interpretation of TCR signal strength[24]. In addition, modulating inflammation did not overcome loss of BATF suggesting that the phenotype was either independent or upstream of inflammatory signaling (Supplementary Fig. 4d-f). Thus, the defects in effector CD8$^+$ T cell responses in the absence of BATF were cell intrinsic and profound.

We next examined the phenotype and function of effector CD8$^+$ T cells generated in the absence of BATF in the mixed P14 chimeras. We found that $Batf^{-/-}$ effector CD8$^+$ T cells showed a higher frequency of CD127^{hi}KLRG1^{lo} memory precursors[10] compared to their wild-type counterparts (Fig. 2c), suggesting that the KLRG1^{hi} phenotype upon direct infection of $Batf^{-/-}$ mice was due to prolonged viral infection and/or CD8$^+$ T cell extrinsic effects (Fig. 1d and Supplementary Fig. 1a). However, while $Batf^{-/-}$ and wild-type effector P14 cells showed similar granzyme B expression, the few $Batf^{-/-}$ effector P14 cells remaining at d8 p.i. produced less IFN-γ, TNF, and IL-2 upon restimulation (Fig. 2d)[3], suggesting altered functionality of effector CD8$^+$ T cells lacking BATF. To examine the underlying mechanisms that account for the altered differentiation of the surviving $Batf^{-/-}$ P14 cells, we analyzed T-bet, Eomes and IRF4 expression. At d8 p.i., virus-specific effector CD8$^+$ T cells displayed lower amounts of Eomes and increased IRF4 in the absence of BATF while they maintained comparable expression of T-bet (Fig. 2e), though because of the low number of $Batf^{-/-}$ effector CD8 T cells it is unclear whether this phenotype is a

function of the selection of the few aberrantly activated survivors. The general effects of *Batf* deficiency on gene expression in the majority of cells may be difficult to assess in this small surviving minority.

Next, we tested whether BATF was required for a secondary effector CD8+ T cell response. Primary *Batf*−/− and wild-type memory P14 cells were generated in separate hosts. At d51 p.i., *Batf*−/− and wild-type memory CD8+ T cells were purified and equal numbers of each genotype were co-transferred into secondary hosts. These recipient mice were then infected with either Listeria (LMgp33) or LCMV Arm. On d7 after re-challenge, the secondary effector response of *Batf*−/− CD8+ T cells was markedly reduced compared to wild-type cells (Fig. 2f). Thus, while some *Batf*−/− CD8+ T cells can apparently enter the memory pool after primary infection and *Batf*−/− memory P14 cells retain a wild-type phenotype (Supplementary Fig. 3d), *Batf*−/− memory CD8+ T cells are also highly defective in secondary effector differentiation. BATF is therefore required for primary and secondary effector CD8+ T cell differentiation.

Restoring BATF rescues *Batf*−/− effector differentiation

We next tested whether the defects in effector differentiation in BATF-deficient CD8+ T cells could be reversed by re-introducing BATF. We used retroviral (RV) transduction in *Batf*−/− and wild-type P14 CD8+ T cells to express BATF and transferred the transduced cells into infection-matched recipients (Supplementary Fig. 5). Re-introducing BATF into *Batf*−/− cells restored the magnitude of the effector CD8+ T cell response and corrected differentiation such as the skewed ratio of memory precursors to short lived effector cells[10] (Fig. 3a-d). In contrast, overexpression of BATF in wild-type CD8+ T cells did not change the number, phenotype or function of CD8+ T cells, suggesting that in wild-type effector CD8+ T cells, BATF expression was not limiting. We found that *Batf*−/− cells were strongly dependent on RV-expressed BATF, as the BATF-transduced *Batf*−/− cells had a major advantage in persistence compared with the non-transduced *Batf*−/− cells (Fig. 3c). Thus, the defect in effector differentiation in *Batf*−/− CD8+ T cells can be overcome by restoring BATF expression. These results further support an intrinsic role of BATF in the CD8+ T cell effector response.

BATF, IRF4, and Jun proteins co-bind target genes

To determine the mechanisms for the profound effect of loss of BATF on effector differentiation, we assembled a map of TF-DNA interactions using ChIP-seq with antibodies against BATF, IRF4, c-Jun, JunD, and JunB in effector CD8+ T cells generated *in vitro*. These *in vitro* effector CD8+ T cells show a similar global transcriptional profile to effectors generated *in vivo* during LCMV infection (Supplementary Fig. 6). To define the chromatin state of TF-bound regions, we also performed ChIP-seq with antibodies to five histone modifications: histone H3 lysine 4 monomethylation (H3K4me1), primarily associated with enhancers; H3K4me3, associated with promoters; H3 lysine 27 acetylation (H3K27ac), found in active regulatory regions; H3K36me3, found in transcriptionally active regions; and H3K27me3, a modification found in Polycomb-repressed regions[25].

We identified high-confidence binding regions for each TF (Fig. 4a and c; and Supplementary Fig. 7a). Examining the chromatin state of the TF-bound regions, we found that all five TFs exhibited a high fraction of peaks in active *cis* regulatory regions, with a strong preference for enhancers over promoters, and very little binding in Polycomb-repressed chromatin (Supplementary Table 1 and Fig. 4b).

A global analysis of BATF- and IRF4-bound genes in effector CD8^{+} T cells revealed a highly significant overlap of regions bound by the two TFs (Fig. 4c), which almost exclusively bound in close proximity (Fig. 4d). Fully 80% of BATF-bound regions had an IRF4-bound region within 1 kb (Fig. 4c and d). However, there was no strong predilection for which Jun family member associated with BATF-bound regions, and each was significantly associated with BATF (Supplementary Fig. 7a). Co-binding with BATF significantly increased the binding density of IRF4 (compared to IRF4-only regions), but co-binding of BATF and IRF4 had no effect on the DNA binding of BATF (Supplementary Fig. 7b and c), suggesting that for IRF4, co-binding with BATF may potentiate TF-DNA interaction strength.

We performed a *de novo* motif analysis of regions bound by BATF and IRF4, or those bound by either BATF or IRF4 alone. The combined BATF-IRF4 sites were highly enriched for both types of the previously described AP-1 ISRE composite element (AICE)[20, 21, 22] (Fig. 4e). In contrast, BATF-only peaks were enriched for only the AP-1 binding motif. However, the IRF4-only peaks also enriched for AP-1 and AICE motifs, perhaps suggesting that IRF4 may cooperatively bind DNA with other members of the AP-1 family in effector CD8^{+} T cells (Fig. 4e). We also found that regions bound by BATF in effector CD8^{+} T cells and in T_H17 cells show an unexpected degree of similarity given the disparate natures of the two cell types (Supplementary Table 2). Thus, BATF together with its dimerization partners c-Jun, JunB, and JunD binds extensively in effector CD8^{+} T cells, largely in combination with IRF4, at motifs enriched for AICEs.

BATF and IRF4 dynamically regulate effector genes

We identified BATF 'target genes' as those with BATF-bound regions within a window spanning the gene and extending 5kb in both 5' and 3' directions. Inspection of these BATF target genes revealed a large number of genes with functions critical for CD8^{+} T cell effector differentiation (Table 1). BATF bound to regulatory regions in the genes encoding many TFs with previously known roles in regulating effector CD8^{+} T cell differentiation, including *Tbx21*[9, 10], *Eomes*[8, 9], *Prdm1*[12,11], and *Id2*[13]. BATF targets included genes involved in T cell receptor (TCR) signaling (*Cd28, Cd3d, Csk) as* well as genes controlling the response to inflammation, such as multiple *Stats*, Il12rb1, Il12rb2, Il18rap, Ifngr2, Il6st, Ifnar1, Ifnar2, and *Il1r1*. BATF also bound to genes that are required for effector function (e.g. *Gzmb, Ifng, Il2*), homing (e.g. *Sell, Selp, Ccr9*), apoptosis (e.g. *Bcl2, Bcl2l1, Mcl1*), and metabolism (e.g. *Gsk3a*, *Rptor*, *Rps6ka1*), suggesting a major role for BATF in regulating critical effector CD8^{+} T cell genes.

We analyzed our previously published gene expression data from naive, effector and memory CD8^{+} T cells[2] and determined whether BATF target genes were overrepresented among genes differentially expressed during effector and memory differentiation. BATF

target genes represented 11 - 17% of all genes that were differentially expressed between naive vs. effector or naive vs. memory CD8^{+} T cells (data not shown), a highly significant over-representation in the transcriptional program of effector/memory differentiation (Fig. 5a). The greatest enrichment in BATF target genes was in those differentially expressed between naive CD8^{+} T cells and any subsequent time-point in effector/memory differentiation (Fig. 5a). This was consistent with early upregulation of BATF and with the profound requirement for BATF in the naive to effector transition (Fig. 2a and b). Thus, BATF binds to a set of functionally critical genes that are dynamically regulated during effector and memory differentiation.

Combinations of TFs regulate temporal gene expression

Because BATF binds to regulatory regions in combination with IRF4, JunB, cJun and JunD, we tested whether the kinetics of BATF target-gene expression during effector/memory differentiation varied depending on whether BATF target-genes were also bound by IRF4 or Jun family members. We first mapped genome-wide combinatorial binding patterns of all five TFs studied, by merging TF binding regions for BATF, IRF4, c-Jun, JunB, and JunD that were in close proximity to each other to define seven clusters of regions bound by combinations of TFs (Fig. 5b). The majority of BATF-bound regions were co-bound by IRF4 and one of the Jun family members (region clusters 3 - 5). However, some regions were associated only with BATF (cluster 1) or only IRF4 (cluster 2). Several clusters (clusters 6 and 7) were also identified consisting of regions bound by Jun family members independent of BATF, possibly representing targets of canonical AP-1 complexes.

Next, we separately identified three broad temporal patterns of gene expression (Fig. 5c) during effector/memory CD8^{+} T cell differentiation. The first pattern (Pattern A) showed a gradual upregulation during differentiation and was enriched for genes classified by Gene Ontology[26] as involved in lymphocyte activation (P=1.4e-2 by hypergeometric test) and migration (P=1.83e-2). A second (Pattern B) included genes transiently upregulated in effectors, and was enriched for genes involved in mitosis (P=7.14e-9) and cell cycle regulation (P=9.9e-9). Finally, a third pattern (Pattern C) included genes initially downregulated in effectors but with gradually recrudescent expression in memory CD8^{+} T cells and was enriched for genes involved in lymphocyte co-stimulation (P=3.01e-4) and lymphocyte differentiation (P=1.33e-3).

We then tested whether the genes bound by specific combinations of TFs defined in Fig. 5b were associated with particular temporal patterns of gene expression defined in Fig. 5c. Genes bound by BATF or IRF4 alone (clusters 1 and 2 from Fig. 5b) were not significantly enriched in any temporal pattern (Fig. 5d). However, genes bound by BATF and IRF4 with or without Jun family members (clusters 3 and 4) were significantly enriched in gene expression pattern A and C – i.e. those genes involved in T cell activation and differentiation. In contrast, BATF and IRF4 with or without Jun target genes were significantly depleted in pattern B – i.e. proliferation-associated genes that were transiently upregulated in effectors but returned to baseline levels during the memory phase. Genes bound by Jun family members without BATF or IRF (cluster 7) showed a reciprocal pattern, with significant enrichment in pattern B and depletion from patterns A and C, consistent

with a role for canonical AP-1 regulation of immediate early genes and those involved in proliferation[27]. Thus, BATF-bound genes were restricted to a specific temporal sequence by the co-binding of other TFs. Genes co-bound by BATF, IRF4, with or without Jun family TFs remained differentially expressed after naive T cells differentiate into effectors (patterns A and C). In contrast, genes that were transiently upregulated and then revert to the low-level expression (pattern B) tended not to include BATF target genes, but were instead enriched for AP-1 target genes. Thus, the kinetics of gene expression during effector and memory CD8$^+$ T cell differentiation was temporally regulated by different combinations of BATF, IRF4 and Jun binding events.

Loss of BATF perturbs the expression of a network of TFs

To identify genes whose expression was altered by BATF loss, we compared the gene expression profiles of naive $Batf^{-/-}$ and wild-type CD8$^+$ T cells and effectors of each genotype generated after *in vitro* activation for three days (Fig. 6a). We found that the profiles of $Batf^{-/-}$ and wild-type effector CD8$^+$ T cells showed marked differences (Fig. 6a). In contrast, the expression profiles of naive wild-type or $Batf^{-/-}$ CD8$^+$ T cells were more closely related, consistent with the phenotypic analyses (Supplementary Fig. 2a). As expected, BATF target genes where highly enriched for genes perturbed by BATF loss (P=9.1e-22).

Inspection of the list of genes perturbed by BATF loss revealed two striking features. First, we found that genes involved in effector function (e.g. *Prf1* and *Ifng*) were significantly increased in expression in $Batf^{-/-}$ effectors, suggesting that BATF inhibits the expression of these genes (Fig. 6b). Second, we found that the expression of a striking number of TFs was perturbed by loss of BATF (Fig. 6b and c). To visualize the network of TFs with which BATF interacts, we combined our BATF ChIP-Seq data, expression profiles of $Batf^{-/-}$ CD8$^+$ T cells, and published data of TF binding patterns (see Methods) to create an interaction network. The network analysis revealed a dense set of interconnected relationships between BATF and a large set of TFs mediated by direct binding, mutual regulation, and shared target genes (Fig. 6c and Supplementary Fig. 8). Many of these interacting TFs were up- or down-regulated in BATF-deficient effectors, suggesting that they were directly regulated by BATF (Fig. 6c). Other TFs bound by BATF did not change in expression in BATF-deficient effectors (Supplementary Fig. 8, shown in gray color in outer circle) suggesting that BATF regulated their expression at a different time point or that their expression was regulated by BATF in combination with other TFs. Many of the TFs that were perturbed by BATF loss have known, critical roles in effector CD8$^+$ T cell differentiation. We identified a lack of induction or downregulation of Id3, T-bet (encoded by *Tbx21*), Blimp-1 (encoded by *Prdm1*) and Runx3 in $Batf^{-/-}$ effectors at early time points after activation, suggesting that BATF reinforces effector CD8$^+$ T cell differentiation by inducing the expression of these TFs. BATF loss increased Eomes expression, potentially pointing to a role for BATF in ensuring the reciprocal expression of T-bet and Eomes that we have recently observed in CD8$^+$ T cells[28]. We found that $Batf^{-/-}$ effector CD8$^+$ T cells showed increased expression of IRF4 and cJun which suggests that BATF may provide negative feedback on the expression of these binding partners.

BATF is required early during effector differentiation

The binding of BATF to a broad set of genes critical to effector CD8$^+$T cell differentiation suggests that BATF may play an essential role at the earliest stages of effector differentiation to specify the key properties of effector CD8$^+$ T cells. To test this idea we tracked effector CD8$^+$ T cell differentiation during the first 96 hours after LCMV infection in *Batf*$^{-/-}$ and wild-type P14 CD8$^+$ T cells. Wild-type CD8$^+$ T cells started to proliferate by d2 p.i. and entered an exponential proliferation state (Fig. 7a and b). In contrast, although *Batf*$^{-/-}$ P14 cells also initiated proliferation with similar kinetics (Fig. 7a), they showed a dramatic collapse in cell number at d4 p.i., suggesting a key role for BATF in coordinating the earliest events in the naive to effector transition for CD8$^+$ T cells. *Batf*$^{-/-}$ CD8$^+$ T effector cells exhibited higher caspase activity (FLICA) and CD95 (*Fas*) expression and lower Bcl-2 expression (Fig. 7c and Supplementary Fig. 9a), suggesting increased cell death as a cause for the collapse during proliferative expansion. It should be noted that a small number of cells appear to survive this collapse in clonal expansion at d4 p.i. and these cells may give rise to the small number of effector CD8 T cells observed at d8 p.i. (see Figs. 1 and 2).

To test whether BATF binding could occur at this early stage of effector CD8$^+$ T cell differentiation, we analyzed the time-course of BATF:DNA interactions at four regions in representative target genes using ChIP-PCR (Supplementary Fig. 9b). BATF bound to all 4 genes examined starting at d1, indicating that binding of BATF to genes involved in effector CD8$^+$ T cell differentiation can take place at the earliest stages (i.e. within 24 hrs) after activation.

One key feature of the naive to effector transition for CD8$^+$ T cells is a switch from a mainly catabolic metabolism for naive T cells to the anabolic or glycolytic metabolic program required to support exponential proliferation and synthesis of biomass that accompanies blastogenesis and rapid division as well as production of effector molecules. We hypothesized that activated CD8$^+$ T cell fail to make these metabolic changes in the absence of BATF. Indeed, at d3 p.i., prior to the proliferative collapse, *Batf*$^{-/-}$ P14 cells displayed reduced cell size (FSC) (Fig. 7a). Moreover, *Batf*$^{-/-}$ CD8$^+$ T cells showed decreased expression of key nutrient transporters or receptors (CD71 and CD98), altered reactive oxygen production (as determined by lower CellROX Deep Red staining) consistent with mitochondrial changes and lower phosphorylation of the S6 ribosomal protein downstream of mTOR (Fig. 7d), indicating a role for BATF in metabolic reprogramming that accompanies effector CD8$^+$ T cell differentiation.

Despite these profound defects, B*atf*$^{-/-}$ P14 cells initially upregulated CD25 and CD69 expression to a degree similar to wild-type P14 cells, suggesting that TCR-dependent early activation events were preserved in the absence of BATF (Supplementary Fig. 9c). However, *Batf*$^{-/-}$ P14 cells showed impaired upregulation of T-bet (Fig. 7e) and failed to up-regulate CD212 (IL12Rβ1) and CD218a (IL18Rα). The defect in CD212 (IL12Rβ1) and CD218a (IL18Rα) protein expression at d2 p.i. preceded the defect in T-bet protein expression at d3 p.i. (Fig. 7e and f). Thus, BATF likely controls T-bet expression at these early time points both through a direct regulatory effect on the gene and, potentially, through

an indirect effect via inflammatory cytokines such as IL-12 that are known inducers of T-bet[7, 10]. At later time points, T-bet expression in the few surviving $Batf^{-/-}$ cells present at d8 p.i. (see Fig. 1) may be driven by an altered inflammatory environment. In addition, $Batf^{-/-}$ cells also failed to upregulate co-stimulatory molecules such as CD30 and CD134 (OX-40) (Supplementary Fig. 9d). These results indicate that BATF plays an essential role in integrating signals 1, 2 and 3 of T cell activation.

Despite the failure to efficiently induce upstream effector transcription factors and cytokine receptors, downstream effector genes were paradoxically upregulated in the absence of BATF early after activation. At d3 p.i. $Batf^{-/-}$ cells displayed inappropriately high expression of CD69 and CD62L (Fig. 7g and Supplementary Fig. 9c). This difference was not due to altered proliferation kinetics of $Batf^{-/-}$ P14 effectors as expression levels of CD62L and CD69 in successive generations of proliferating effectors were different between $Batf^{-/-}$ and wild-type early effectors (Supplementary Fig. 9e). In addition, $Batf^{-/-}$ cells produced more IFN-γ and granzyme B (Fig. 7h), both direct targets of BATF (Fig. 4f and 6b), with similar trends for other effector cytokines such as TNF and MIP-1α (Supplementary Fig. 9f). These observations indicate that while BATF is necessary to induce key positive regulators of effector CD8+ T cell differentiation including TFs and cytokine receptors, BATF also represses the downstream effector gene targets. These results suggest that BATF is a critical component of a feed-forward transcriptional circuit that coordinates the gene expression program of effector CD8+ T cells differentiation (Supplementary Fig. 10). A key feature of this model is dual induction of upstream regulators of effector CD8+ T cell differentiation (e.g. TF and cytokine receptor genes) and repression of downstream effector gene targets (e.g. IFN-γ, granzyme B) ensuring that effector CD8+ T cell differentiation is not 'locked in' until a sufficient threshold of upstream signals is achieved to overcome this latter BATF repression.

Discussion

Several studies have found that BATF regulates T_H17 and T_{FH} cell differentiation[14, 16, 17], but its role in CD8+ T cells remains poorly understood. BATF represses effector function in exhausted CD8+ T cells[19] and regulates metabolism and/or epigenetics in CD8+ T cells via Sirt1[29]. Here, we show that BATF orchestrates the developmental transition from naive to effector states in CD8+ T cells. Our data identify BATF as a checkpoint in a transcriptional circuit that ensures proper coordination of effector CD8+ T cell differentiation. In this circuit, BATF serves two distinct and critical functions. First, it directly upregulates critical TFs associated with the acquisition of effector functions including T-bet, Runx3 and Blimp-1, as well as cytokine receptors and STAT TFs that sense inflammation and reinforce effector differentiation. Second, BATF binds to and/or represses the expression of downstream effector molecules, such as IFN-γ, perforin and granzyme B. Without BATF, the coordinated sequence of molecular events that occur during effector CD8+ T cell differentiation is disrupted, and effector CD8+ T cells reach a differentiation crisis marked by metabolic and proliferative catastrophe within 3 - 5 days of antigen encounter.

Several TFs regulate effector CD8+ T cell differentiation[7]. Naive CD8 T cells lacking either T-bet[9, 10], Blimp-1[11], Id2[13] or Runx3[30] show defects in the magnitude of the effector

response, as well as reduced cytotoxic potential or IFN-γ expression. However, the mechanism that coordinates the upregulation of this set of TFs has been unclear. We find that BATF directly or indirectly regulates a dense network of transcription factors, including many TFs known to be required for effector CD8^{+} T cell differentiation. In the absence of BATF, the early upregulation of its target genes, T-bet, Runx3 and Blimp-1 is impaired, indicating that BATF may function upstream of each of these TFs to regulate their appropriate temporal induction during effector CD8^{+} T cell differentiation. In addition to directly upregulating these effector TFs, BATF also binds to and/or upregulates *Ifnar1*, *Ifnar2*, *Il12rb1*, and *Il12rb2*, inflammatory cytokine receptors that positively reinforce expression of *Tbx21* and effector genes[10]. Thus, BATF integrates Signal 1 (TCR-mediated activation) and Signal 3 (inflammatory cytokine sensing) of T cell activation to ensure commitment to an effector fate.

It may seem counter-intuitive that BATF both positively regulates effector TFs while negatively regulating downstream effector molecules, such IFN-γ, perforin and granzyme B. However in bacteria, yeast, and cell lines, circuits involving opposing actions on downstream genes (termed incoherent feed-forward loops) are a common[31][32, 33]. BATF positively regulates lineage-specific TFs as well as the inflammatory cytokine receptors (*Ifnar1*, *Ifnar2*, *Il12rb1*, and *Il12rb2*) that are known to reinforce *Tbx21* and other effector genes[10]. The negative arm represses effector molecules (IFN-γ, perforin and granzyme B) thus forming an incoherent feed-forward loop. Such loops can serve as 'persistence detectors' that suppress an inappropriate response to a transient or subthreshold burst of stimulation, and delay downstream gene expression until a full-fledged stimulus occurs[33]. The simultaneous repression of effector genes by BATF ensures that the full effector program is 'locked in' only when the positive regulatory arms have reached a critical threshold to overcome the downstream inhibition mediated by BATF at effector genes. The essentiality of this coordinated deployment of effector functions is demonstrated by the early and profound collapse of effector CD8^{+} T cell differentiation in the absence of BATF.

BATF expression is increased in exhausted T cells during chronic viral infections in humans and mice[19]. In this setting, the primary function of BATF seems to be to repress effector genes such as IFN-γ. The dual role we describe for BATF in early T cell activation, however, suggests that it may be possible to distinguish the distinct effects of BATF on inducing a differentiation program (as BATF does in effector differentiation) from effects on modulating gene expression once that program is established (as it does in exhausted CD8^{+} T cells). Such an interpretation would suggest that once CD8^{+} T cells progress past the point of initial effector differentiation, BATF tunes functionality depending on the strength and/or duration of TCR stimulation. Future studies temporally removing BATF at different stages of infection should reveal further insights into the potential context-specific functions of BATF.

Two previous studies demonstrated that IRF4 is regulated in a TCR signal-strength dependent fashion and is required for effector CD8^{+} T cell differentiation[24, 34]. Consistent with these findings, we show that BATF and IRF4 co-operate to regulate effector CD8^{+} T cell differentiation. The regions bound by BATF and IRF4 overlap extensively and the two TFs bind in close proximity at regions enriched for the composite AICE motif largely

consistent with recent data from studies of Th17 cells[20, 35, 21, 22]. We show that BATF and IRF4 co-binding is functionally co-operative: only genes bound by both TFs (but not those bound only by one) are dynamically regulated during effector differentiation suggesting that the association of both TFs is required to execute the differentiation program. Although BATF is also upregulated in response to TCR signaling[19], we show that availability of BATF was not limiting in wild-type CD8^{+} T cells because overexpression of BATF did not further enhance effector differentiation. Moreover, loss of only a single allele of *Batf* demonstrated that sufficient BATF protein was available for effector CD8^{+} T cell differentiation even in the heterozygous setting. Thus, the role of IRF4 may be to contribute a signal-strength sensing component to the activity of the BATF-IRF4 complex[24]. Such TCR-signal-induced upregulation of IRF4 is balanced by negative regulation of IRF4 by BATF, providing a feedback mechanism that limits the effect of this TF complex and prevents overstimulation during effector CD8^{+} T cell activation.

Why do BATF deficient effector cells die? BATF deficient effectors are able to enter cell cycle, but fail to increase in number. This phenotype is reminiscent of CD8^{+} T cells that are unable to sense inflammatory cytokines such as IFN-I[36]. However, we found that modulation of inflammation did not alter the response of BATF-deficient CD8^{+} T cells, perhaps because these cells fail to express appropriate levels of cytokine receptors. During effector differentiation, CD8^{+} T cells must undergo a metabolic reprogramming, shifting to an anabolic program that accompanies massive proliferation and increase in biomass[4]. *Batf*^{−/−} CD8^{+} T cells fail to manifest several important components of this metabolic shift including increase in cell size, upregulation of nutrient transporters, optimal mTOR activation and mitochondrial function. These changes could be due to disruption of downstream genes involved in regulating metabolism, as has been reported for IRF4[24] and BATF[29]. Alternatively or in addition, dysregulation of a large network of TFs, cytokine receptors, and effector genes in the absence of BATF may be perceived as a developmental catastrophe, triggering an apoptotic response preceded by disordered metabolism. Future work should address whether enforced expression of specific, individual BATF target genes could rescue the defect in effector differentiation. However, given the broad range of critical genes regulated by BATF, it may be that no single gene is capable of restoring normal effector differentiation in the absence of BATF.

Several questions regarding the role of BATF in regulating effector differentiation remain. BATF is required for differentiation of T_H17 and T_{FH} cells[14, 16]. Our data examining effector CD8^{+} T cells now reveal that BATF orchestrates the transition from naive to effector CD8^{+} T cells and suggest that BATF has a broad role across many lymphocyte lineages. It remains unclear, however, how BATF can be required for diverse differentiation programs in different cells. BATF functions as a 'pioneer factor' in T_H17 cells, increasing chromatin accessibility to allow subsequent binding by other TFs[22]. BATF may therefore lay 'foundation' of open regulatory regions on top of which additional layers of regulation are added through the combined action of stimulus-specific TFs such as STATs[37] and effector TFs such as T-bet and Blimp-1. Future studies will be required to define the 'parts list' of TFs that contribute to each lineage, and to determine how their layered, combinatorial binding with BATF-IRF4 shapes the identity of developing effector cells.

Online Methods

Mouse

C57Bl/6 background *Batf*^{−/−} mice were purchased from the Jackson laboratory[14]. C57Bl/6 (CD45.2[+]) and congenic (CD45.1[+]) mice were from the National Cancer Institute. For some of the experiments, they were crossed to P14 TCR transgenic mice. Male mice were used at between 5 and 10 weeks of age. All animal work was in accordance with the Institute Animal Care and Use Guidelines for the University of Pennsylvania.

Infection and immunization

LCMV strains were produced and titers were measured as described[38]. Mice were infected by intraperitoneal injection of LCMV Armstrong strain (2×10^5 plaque-forming units). In some experiments, mice were infected by intravenous injection of *Listeria monocytogenes* expressing LCMV gp33 epitope (LMgp33; 1×10^4 colony-forming units or immunized by intravenous injection of bone marrow derived dendritic cells labeled with gp33 peptide (DCgp33; 1×10^6 cells)[39].

Adoptive transfer and isolation of lymphocytes

For adoptive transfer of naive cells, CD8^{+} T cells were isolated from spleens of naive *Batf*^{−/−} or wild-type P14 mice by CD8 negative selection (Miltenyi Biotec). The indicated number (1×10^3–10^6) of 1:1 mixed, or single P14 cells, were transferred into nonirradiated naive recipient mice. For proliferation assays, P14 cells were labeled with 10μM CFSE or Cell Trace Violet (Invitrogen) before transfer. For flow cytometry analysis after infection, major lymphoid and non-lymphoid organs were removed on the days indicated, and single cell suspensions were prepared as previously described[39]. RBCs in the cell suspensions were lysed using ammonium chloride. To transfer memory P14 cells, *Batf*^{−/−} and wild-type memory P14 cells were generated in the two groups of mice. Spleen cells containing P14 cells were isolated, mixed and transferred into new recipient mice.

Retrovirus production and transduction

Batf cDNA was cloned into the MIG retrovirus[38]. Empty MIG or BATF-expressing MIG was produced in 293T cells by the calcium-phosphate methods. For retrovirus transduction, naive *Batf*^{−/−} and wild-type P14 cells were isolated from spleen cells and enriched by CD8 negative selection. After 24 hours activation with anti-CD3 (2C11; 1μg/ml) and anti-CD28 (37.51; 0.5μg/ml) antibodies in the presence of recombinant human IL-2 (100 U/ml), P14 cells were transduced with retrovirus supernatant containing polybrene (1 μg/ml) by spin infection (2000*g* for 60 min at 30°C). After 4 hours incubation, RV-transduced P14 cells were adoptively transferred into recipient mice that were infected with LCMV Arm one day before.

Antibodies and flow cytometry

The following fluorochrome-conjugated antibodies were used: TCR Vα2 (B20.1), CD8a (53-6.7), CD25 (PC61.5), CD27 (LG.3A10), CD29 (HMβ1-1) CD43 (1B11), CD45.1 (A20), CD45.2 (104), CD62L (MEL14), , CD69 (H1.2F3), CD71 (R17217), CD122 (5H4 and TM-

β1), CD127 (A7R34), CD132 (TUGm2), CD183 (CXCR3; 173), CD218a (BG/IL18RA), Ly6C (HK1.4), KLRG1 (2F1), , T-bet (4B10), IL-2 (JES6-5H4) from Biolegend; CD30 (mCD30.1), CD44 (IM7), CD95 (15A7), CD134 (OX-86), Eomes (Dan11mag), IRF4 (3E4), IFN-γ (XMG1.2) , TNF (MP6-XT22), BATF (MBM7C7) from eBioscience; Bcl-2 (3F11), CD162 (PSGL1; 2PH1), CD212 (114) from BD Phamingen; Granzyme B (GB12) from Invitrogen; MIP1α(39624) from R&D; Phospho-S6 (Ser235/236) (91B2) from Cell Signaling Technology. MHC class I H-2D^b gp33 tetramers were described previously[38]. MHC class II I-Ab gp66 tetramers were obtained from the National Institute of Health Tetramer Core. Aqua live dead staining (Invitrogen) was used for exclusion of dead cells. Assessment of caspase activity and reactive oxygen species production was performed using FLICA Poly Caspases Assay kit (Immunochemistry Technologies) and CellROX assay kit (Invitrogen). For intracellular cytokine staining, single cell suspension was incubated with or without 1 μM gp33 peptide in the presence of brefeldin A and IL-2 (100 U/ml) for 5 h at 37°C and stained using the Cytofix/Cytoperm kit (BD). For intracellular transcription factor staining, Foxp3 staining kit (eBioscience) was used according to manufacturer's instruction. Samples were analyzed on an LSRII (BD) and data were analyzed with FlowJo software (Tree Star).

In vitro Stimulation and Differentiation

Primary wild-type and *Batf*$^{-/-}$ P14 CD8$^+$ T cells were isolated using CD8 negative selection magnetic-activated cell sorting (MACS) kits (Miltenyi) and cultured in RPMI 1640 supplemented with 10% fetal bovine serum, 10 mM HEPES, 50 U/ml of Penicillin, 50 μg/ml of Streptomycin, and 50 μM β-mercaptoethanol. Naive cells were stimulated with plate-bound anti-CD3 (4 μg/ml, clone 2C11, BD Pharmingen) and anti-CD28 (4 μg/ml, clone 37.51, BD Pharmingen) in the presence of recombinant human IL-2 (100 U/ml, R&D Systems) for 3 days to generate *in vitro* effector cells.

Chromatin immunoprecipitation

In vitro effector CD8$^+$ T cells were fixed with 1% formaldehyde for 10 min at 37°C. The cells were then washed twice in ice cold PBS, and the cell pellets were flash frozen and stored at −80°C. For each transcription factor ChIP, 10 or 20×10^6 cells were used, and 1.5×10^6 cells were used for each histone ChIP. The fixed cells were resuspended in 120 μl of lysis buffer (0.5% SDS, 50 mM Tris, pH 8, 10 mM EDTA, 1x Complete protease inhibitor (Roche)) per 5×10^6 cells (or a minimum 120 μl of lysis buffer for less than 5×10^6 cells), and the chromatin was sheared using a Covaris E210 Ultrasonicator (Covaris, Inc.) and Covaris microTUBEs. Each microTUBE (120 μl of lysate) was sonicated with 6 treatments of 60 sec each with the following settings: Intensity of 5, Duty Cycle of 10 %, and 200 Cycles per Burst. This sonication sheared the chromatin into fragments of 150-600 bp, with the majority of DNA fragments being 200-250 bp in length. The sonicated lysates were collected and centrifuged for 10 min at 4°C. Supernatants were collected and 4 parts of dilution buffer (1.25% Triton X-100, 12.5 mM Tris, pH 8, 187.5 mM NaCl, 1x Complete protease inhibitor) were added. Immunoprecipitation was performed overnight using Dynabeads Protein G (Life Technologies) pre-bound to 5 μg of specific antibodies. The following antibodies were used for ChIP: anti-BATF (PAB4003, Lot #004, Brookwood Biomedical), anti-IRF4 (M-17) (sc-6059, Lot #C2712), anti-cJun (N) (sc-45, Lot #K3010),

anti-JunB (210) (sc-73, Lot #D2610), anti-JunD (329) (sc-74, Lot #I1510, Santa Cruz), anti-Total H3 (ab1791, Lot #GR82485), anti-H3K4me1 (ab8895, Lot #GR61280), anti-H3K4me3 (ab8580, Lot #GR33084), anti-H3K27ac (ab4729, Lot #GR52136), anti-H3K36me3 (ab9050, Lot #GR36719, Abcam), anti-H3K27me3 (07-449, Lot #2064519, Millipore), and Normal Rabbit IgG (Control IgG) (10500C, Lot #939223A, Life Technologies). Precipitated immune complexes were then washed once with Low Salt Buffer (0.1% SDS, 1% Triton X-100, 20m M Tris, pH 8, 2 mM EDTA, 150 mM NaCl, 1x Complete protease inhibitor), once with High Salt Buffer (0.1% SDS, 1% Triton X-100, 20m M Tris, pH 8, 2 mM EDTA, 500 mM NaCl, 1x Complete protease inhibitor), twice with LiCl Buffer (0.7% Sodium Deoxycholate (NaDOC), 1% NP-40, 20m M Tris, pH 8, 1 mM EDTA, 500 mM LiCl, 1x Complete protease inhibitor), and once with TE buffer (with protease inhibitor) for 5 min each. The ChIP immune complexes were then eluted from the beads twice in elution buffer (1% SDS, 0.1 M NaHCO$_3$) with constant agitation for 30 min. The eluates were pooled and incubated at 65°C overnight to reverse the formaldehyde cross-links. The eluates were then treated with 200 μg of RNase A (Qiagen) and 40 μg of Proteinase K (Life Technologies) for 2 hr at 37°C. ChIP DNA fragments were purified using a MinElute Reaction Cleanup kit (Qiagen).

High-throughput Sequencing

ChIP DNA was prepared for high-throughput Illumina sequencing using the NEBNext ChIP-Seq Library Master Mix Set for Illumina kit (New England Biolabs, Inc.) and the NEBNext Multiplex Oligos for Illumina (Index Primers 1-12) kit (New England Biolabs, Inc.) according to a modified manufacturer's protocol. For each ChIP or input sample, 10-50 ng of DNA was used to prepare a sequencing library. The DNA fragments were end-repaired, dA-tailed, and ligated to Illumina adaptors according to the kit instructions. DNA fragments of 150-600 bp in length were then selected using Pippin Prep 2% Agarose Gel Cassettes and the Pippin Prep DNA Size Selection System (Sage Science, Inc.). After each step, the DNA was purified using either a MinElute Reaction Cleanup Kit or a QIAquick PCR Purification Kit (Qiagen), depending on the desired volume for the next step in the library preparation. The ChIP DNA was then amplified with 12 PCR cycles using the NEBNext Multiplex Oligos. Amplified DNA was purified using a 1:1 ratio of DNA to Agencourt AMPure XP beads (Beckman Coulter). The multiplexed DNA libraries were sequenced on the Illumina HiSeq2000. Reads were aligned to the mouse NCBI37/mm9 reference genome using *bowtie*[40], sorted with *samtools*[41], and deduplicated with *picard* (http://picard.sourceforge.net/). *SPP*[42] was used for the generation of visualization tracks for ChIP reads corrected for background (input, IgG or total H3, as appropriate).

ChIP-Seq Informatics

SPP and *MACS2*[43] were both used for peak finding. Regions from both peak callers were combined with *mergeBed*[44]. Quality rating for the merged regions was assigned based on the maximum significance from either source. Independent samples of BATF and IRF4 were generated and sequenced along with their matched input, which were compared to our original samples and their matched inputs, as recommended in the ENCODE ChIP-seq guidelines[45]. We confirmed This sonication sheared the chromatin into fragments of 150-600 bp, with the majority of DNA fragments being 200-250 bp in length. The

reproducibility of the ChIP-seq datasets using the IDR as recommended in the on-line documentation (https://sites.google.com/site/anshulkundaje/projects/idr) on peaks called by *SPP* [42] at FDR < 0.5. At this threshold, SPP reported between 30,000 and 300,000 peaks, depending on the exact combination of sample and input, most of which are expected to be noise. CRMs were identified as in Ciofani et al.[22] except that we used region boundaries for merging rather than summit positions, allowing up to 100 bases between regions. CRMs overlapping repeat-masked sequences (UCSC repeatMasker regions downloaded 8 December 2012) by 67% were removed with *intersectBed −v*[44]. Counts per million for each CRM were determined on deduplicated samples from which "unknown scaffold" alignments had been removed by explicitly retaining only named chromosomes with *samtools* view[41].

Sequences containing overlapping high-confidence BATF and IRF4 binding sites were submitted on-line to the MEME-ChIP server (version 4.9.0)[46] for motif detection using default parameters but with the maximum motif width set at 30. Gene Ontology (GO) annotations were downloaded from NCBI Gene (9 January 2013) and used to assign functional categories to differentially expressed genes and to CRM-associated genes.

Gene expression analysis

Affymetrix Mouse Gene 1.0 ST arrays and associated annotations were downloaded from the NCBI Gene Expression Omnibus (GSE30431 and GPL6246 - December 2012 revision, respectively). Intensities were corrected for background, normalized and log2-converted using R and the *rma* function of the Bioconductor *affy* package[47, 48, 49, 50]. We focused on probe sets annotated to RefSeq genes whose expression was above the overall median expression level in at least 2 samples and which had an interquartile range across all samples > 1.2-fold. Comparisons were carried out pair-wise across time points and *P* value adjustments were made independently for each comparison.

For the analysis of wild-type and *Batf*^{−/−} naive and *in vitro* effector CD8^{+} T cells, the cells were lysed in RLT Buffer, and total RNA was isolated using an RNeasy Mini Kit (Qiagen). After fragmentation and biotinylation, cDNA was hybridized to the Affymetrix Mouse430_2 microarray.

Cluster analysis

We identified three patterns of gene expression during effector/memory CD8 T cell differentiation in our previously published dataset[2] (Fig. 5c) using the k-means algorithm. The value of k was determined automatically as the minimum value that provides within cluster similarity (average correlation with centroid) over a cutoff of 0.8. We computed the overlap between the resultant temporal clusters and the various binding patterns by using a hypergeometric score (estimating the overlap between the respective gene sets). To define gene sets associated with a certain binding pattern, we associate each CRM with its nearest gene.

Defining the BATF-centric network

Key transcriptional interactions involving BATF were computed based on profiles of protein-DNA binding activity and mRNA expression changes under various perturbations.

To identify BATF-outgoing edges we used the knockout and ChIP-seq data collected in this study. BATF-incoming edges were obtained from[51, 52, 53, 54, 55, 56] for physical interactions and [14, 57, 58, 59, 60, 61, 62, 63] for functional effects (using a 1.5 fold change cutoff), as described in[64]. TF that share a significant amount of target genes with BATF were identified using a hypergeometric test with a cutoff of 1e-5.

Statistics

All mice and samples that had entered experiments were analyzed. No pre-experiment statistical methods, randomization or blinding were used in animal experiments. Sample-size choice and assumption of normality were based on similar analyses in published studies. A unpaired Student's *t*-test (two-tailed) was done to assess statistical significance in flow cytometry data. Prism 5 (GraphPad Software) was used to calculate statistics. Results were considered significant at $P < 0.05$.

Supplementary Material

Refer to Web version on PubMed Central for supplementary material.

Acknowledgments

References

1. Kaech SM, Wherry EJ, Ahmed R. Effector and memory T-cell differentiation: implications for vaccine development. Nat Rev Immunol. 2002; 2(4):251–262. [PubMed: 12001996]

2. Doering TA, Crawford A, Angelosanto JM, Paley MA, Ziegler CG, Wherry EJ. Network analysis reveals centrally connected genes and pathways involved in CD8+ T cell exhaustion versus memory. Immunity. 2012; 37(6):1130–1144. [PubMed: 23159438]

3. Kaech SM, Wherry EJ. Heterogeneity and cell-fate decisions in effector and memory CD8+ T cell differentiation during viral infection. Immunity. 2007; 27(3):393–405. [PubMed: 17892848]

4. van der Windt GJ, Pearce EL. Metabolic switching and fuel choice during T-cell differentiation and memory development. Immunol Rev. 2012; 249(1):27–42. [PubMed: 22889213]

5. Rutishauser RL, Kaech SM. Generating diversity: transcriptional regulation of effector and memory CD8 T-cell differentiation. Immunol Rev. 2010; 235(1):219–233. [PubMed: 20536566]

6. Belz GT, Kallies A. Effector and memory CD8+ T cell differentiation: toward a molecular understanding of fate determination. Curr Opin Immunol. 2010; 22(3):279–285. [PubMed: 20434894]

7. Kaech SM, Cui W. Transcriptional control of effector and memory CD8+ T cell differentiation. Nat Rev Immunol. 2012; 12(11):749–761. [PubMed: 23080391]

8. Pearce EL, Mullen AC, Martins GA, Krawczyk CM, Hutchins AS, Zediak VP, et al. Control of effector CD8+ T cell function by the transcription factor Eomesodermin. Science. 2003; 302(5647): 1041–1043. [PubMed: 14605368]

9. Intlekofer AM, Takemoto N, Wherry EJ, Longworth SA, Northrup JT, Palanivel VR, et al. Effector and memory CD8+ T cell fate coupled by T-bet and eomesodermin. Nat Immunol. 2005; 6(12): 1236–1244. [PubMed: 16273099]

10. Joshi NS, Cui W, Chandele A, Lee HK, Urso DR, Hagman J, et al. Inflammation directs memory precursor and short-lived effector CD8(+) T cell fates via the graded expression of T-bet transcription factor. Immunity. 2007; 27(2):281–295. [PubMed: 17723218]

11. Rutishauser RL, Martins GA, Kalachikov S, Chandele A, Parish IA, Meffre E, et al. Transcriptional repressor Blimp-1 promotes CD8(+) T cell terminal differentiation and represses the acquisition of central memory T cell properties. Immunity. 2009; 31(2):296–308. [PubMed: 19664941]

12. Kallies A, Xin A, Belz GT, Nutt SL. Blimp-1 transcription factor is required for the differentiation of effector CD8(+) T cells and memory responses. Immunity. 2009; 31(2):283–295. [PubMed: 19664942]

13. Cannarile MA, Lind NA, Rivera R, Sheridan AD, Camfield KA, Wu BB, et al. Transcriptional regulator Id2 mediates CD8+ T cell immunity. Nat Immunol. 2006; 7(12):1317–1325. [PubMed: 17086188]

14. Schraml BU, Hildner K, Ise W, Lee WL, Smith WA, Solomon B, et al. The AP-1 transcription factor Batf controls T(H)17 differentiation. Nature. 2009; 460(7253):405–409. [PubMed: 19578362]

15. Betz BC, Jordan-Williams KL, Wang C, Kang SG, Liao J, Logan MR, et al. Batf coordinates multiple aspects of B and T cell function required for normal antibody responses. J Exp Med. 2010; 207(5):933–942. [PubMed: 20421391]

16. Ise W, Kohyama M, Schraml BU, Zhang T, Schwer B, Basu U, et al. The transcription factor BATF controls the global regulators of class-switch recombination in both B cells and T cells. Nat Immunol. 2011; 12(6):536–543. [PubMed: 21572431]

17. Murphy TL, Tussiwand R, Murphy KM. Specificity through cooperation: BATF-IRF interactions control immune-regulatory networks. Nat Rev Immunol. 2013; 13(7):499–509. [PubMed: 23787991]

18. Grigoryan G, Reinke AW, Keating AE. Design of protein-interaction specificity gives selective bZIP-binding peptides. Nature. 2009; 458(7240):859–864. [PubMed: 19370028]

19. Quigley M, Pereyra F, Nilsson B, Porichis F, Fonseca C, Eichbaum Q, et al. Transcriptional analysis of HIV-specific CD8+ T cells shows that PD-1 inhibits T cell function by upregulating BATF. Nat Med. 2010; 16(10):1147–1151. [PubMed: 20890291]

20. Glasmacher E, Agrawal S, Chang AB, Murphy TL, Zeng W, Vander Lugt B, et al. A genomic regulatory element that directs assembly and function of immune-specific AP-1-IRF complexes. Science. 2012; 338(6109):975–980. [PubMed: 22983707]

21. Li P, Spolski R, Liao W, Wang L, Murphy TL, Murphy KM, et al. BATF-JUN is critical for IRF4-mediated transcription in T cells. Nature. 2012; 490(7421):543–546. [PubMed: 22992523]

22. Ciofani M, Madar A, Galan C, Sellars M, Mace K, Pauli F, et al. A validated regulatory network for Th17 cell specification. Cell. 2012; 151(2):289–303. [PubMed: 23021777]

23. Wang J, Sun Q, Morita Y, Jiang H, Groß A, Lechel A, et al. A differentiation checkpoint limits hematopoietic stem cell self-renewal in response to DNA damage. Cell. 2012; 148(5):1001–1014. [PubMed: 22385964]

24. Man K, Miasari M, Shi W, Xin A, Henstridge DC, Preston S, et al. The transcription factor IRF4 is essential for TCR affinity-mediated metabolic programming and clonal expansion of T cells. Nat Immunol. 2013; 14(11):1155–1165. [PubMed: 24056747]

25. Ernst J, Kheradpour P, Mikkelsen TS, Shoresh N, Ward LD, Epstein CB, et al. Mapping and analysis of chromatin state dynamics in nine human cell types. Nature. 2011; 473(7345):43–49. [PubMed: 21441907]

26. Ashburner M, Ball CA, Blake JA, Botstein D, Butler H, Cherry JM, et al. Gene ontology: tool for the unification of biology. The Gene Ontology Consortium. Nat Genet. 2000; 25(1):25–29. [PubMed: 10802651]

27. Lau LF, Nathans D. Expression of a set of growth-related immediate early genes in BALB/c 3T3 cells: coordinate regulation with c-fos or c-myc. Proc Natl Acad Sci U S A. 1987; 84(5):1182–1186. [PubMed: 3469660]

28. Paley MA, Kroy DC, Odorizzi PM, Johnnidis JB, Dolfi DV, Barnett BE, et al. Progenitor and terminal subsets of CD8+ T cells cooperate to contain chronic viral infection. Science. 2012; 338(6111):1220–1225. [PubMed: 23197535]

29. Kuroda S, Yamazaki M, Abe M, Sakimura K, Takayanagi H, Iwai Y. Basic leucine zipper transcription factor, ATF-like (BATF) regulates epigenetically and energetically effector CD8 T-cell differentiation via Sirt1 expression. Proc Natl Acad Sci U S A. 2011; 108(36):14885–14889. [PubMed: 21873234]

30. Cruz-Guilloty F, Pipkin ME, Djuretic IM, Levanon D, Lotem J, Lichtenheld MG, et al. Runx3 and T-box proteins cooperate to establish the transcriptional program of effector CTLs. J Exp Med. 2009; 206(1):51–59. [PubMed: 19139168]

31. Yosef N, Regev A. Impulse control: temporal dynamics in gene transcription. Cell. 2011; 144(6): 886–896. [PubMed: 21414481]

32. Mangan S, Itzkovitz S, Zaslaver A, Alon U. The incoherent feed-forward loop accelerates the response-time of the gal system of Escherichia coli. J Mol Biol. 2006; 356(5):1073–1081. [PubMed: 16406067]

33. Mangan S, Alon U. Structure and function of the feed-forward loop network motif. Proc Natl Acad Sci U S A. 2003; 100(21):11980–11985. [PubMed: 14530388]

34. Yao S, Buzo Bruno F, Pham D, Jiang L, Taparowsky Elizabeth J, Kaplan Mark H, et al. Interferon Regulatory Factor 4 Sustains CD8+ T Cell Expansion and Effector Differentiation. Immunity. 2013; 39(5):833–845. [PubMed: 24211184]

35. Tussiwand R, Lee WL, Murphy TL, Mashayekhi M, Wumesh KC, Albring JC, et al. Compensatory dendritic cell development mediated by BATF-IRF interactions. Nature. 2012; 490(7421):502–507. [PubMed: 22992524]

36. Kolumam GA, Thomas S, Thompson LJ, Sprent J, Murali-Krishna K. Type I interferons act directly on CD8 T cells to allow clonal expansion and memory formation in response to viral infection. J Exp Med. 2005; 202(5):637–650. [PubMed: 16129706]

37. Vahedi G, Takahashi H, Nakayamada S, Sun HW, Sartorelli V, Kanno Y, et al. STATs shape the active enhancer landscape of T cell populations. Cell. 2012; 151(5):981–993. [PubMed: 23178119]

38. Kao C, Oestreich KJ, Paley MA, Crawford A, Angelosanto JM, Ali MA, et al. Transcription factor T-bet represses expression of the inhibitory receptor PD-1 and sustains virus-specific CD8+ T cell responses during chronic infection. Nat Immunol. 2011; 12(7):663–671. [PubMed: 21623380]

39. Kurachi M, Kurachi J, Suenaga F, Tsukui T, Abe J, Ueha S, et al. Chemokine receptor CXCR3 facilitates CD8(+) T cell differentiation into short-lived effector cells leading to memory degeneration. J Exp Med. 2011; 208(8):1605–1620. [PubMed: 21788406]

40. Langmead B, Trapnell C, Pop M, Salzberg SL. Ultrafast and memory-efficient alignment of short DNA sequences to the human genome. Genome Biol. 2009; 10(3):R25. [PubMed: 19261174]

41. Li H, Handsaker B, Wysoker A, Fennell T, Ruan J, Homer N, et al. The Sequence Alignment/Map format and SAMtools. Bioinformatics. 2009; 25(16):2078–2079. [PubMed: 19505943]

42. Kharchenko PV, Tolstorukov MY, Park PJ. Design and analysis of ChIP-seq experiments for DNA-binding proteins. Nat Biotechnol. 2008; 26(12):1351–1359. [PubMed: 19029915]

43. Zhang Y, Liu T, Meyer CA, Eeckhoute J, Johnson DS, Bernstein BE, et al. Model-based analysis of ChIP-Seq (MACS). Genome Biol. 2008; 9(9):R137. [PubMed: 18798982]

44. Quinlan AR, Hall IM. BEDTools: a flexible suite of utilities for comparing genomic features. Bioinformatics. 2010; 26(6):841–842. [PubMed: 20110278]

45. Landt SG, Marinov GK, Kundaje A, Kheradpour P, Pauli F, Batzoglou S, et al. ChIP-seq guidelines and practices of the ENCODE and modENCODE consortia. Genome Res. 2012; 22(9): 1813–1831. [PubMed: 22955991]

46. Machanick P, Bailey TL. MEME-ChIP: motif analysis of large DNA datasets. Bioinformatics. 2011; 27(12):1696–1697. [PubMed: 21486936]

47. Team RDC. R: A language and environment for statistical computing. R Foundation for Statistical Computing; Vienna, Austria: 2009.

48. Irizarry RA, Bolstad BM, Collin F, Cope LM, Hobbs B, Speed TP. Summaries of Affymetrix GeneChip probe level data. Nucleic Acids Res. 2003; 31(4):e15. [PubMed: 12582260]

49. Bolstad BM, Irizarry RA, Astrand M, Speed TP. A comparison of normalization methods for high density oligonucleotide array data based on variance and bias. Bioinformatics. 2003; 19(2):185–193. [PubMed: 12538238]

50. Irizarry RA, Hobbs B, Collin F, Beazer-Barclay YD, Antonellis KJ, Scherf U, et al. Exploration, normalization, and summaries of high density oligonucleotide array probe level data. Biostatistics. 2003; 4(2):249–264. [PubMed: 12925520]

51. Linhart C, Halperin Y, Shamir R. Transcription factor and microRNA motif discovery: the Amadeus platform and a compendium of metazoan target sets. Genome Res. 2008; 18(7):1180–1189. [PubMed: 18411406]

52. Zheng G, Tu K, Yang Q, Xiong Y, Wei C, Xie L, et al. ITFP: an integrated platform of mammalian transcription factors. Bioinformatics. 2008; 24(20):2416–2417. [PubMed: 18713790]

53. Wilson NK, Foster SD, Wang X, Knezevic K, Schutte J, Kaimakis P, et al. Combinatorial transcriptional control in blood stem/progenitor cells: genome-wide analysis of ten major transcriptional regulators. Cell stem cell. 2010; 7(4):532–544. [PubMed: 20887958]

54. Lachmann A, Xu H, Krishnan J, Berger SI, Mazloom AR, Ma'ayan A. ChEA: transcription factor regulation inferred from integrating genome-wide ChIP-X experiments. Bioinformatics. 2010; 26(19):2438–2444. [PubMed: 20709693]

55. Liberzon A, Subramanian A, Pinchback R, Thorvaldsdottir H, Tamayo P, Mesirov JP. Molecular signatures database (MSigDB) 3 . Bioinformatics. 2011; 27(12):1739–1740. [PubMed: 21546393]

56. Jiang C, Xuan Z, Zhao F, Zhang MQ. TRED: a transcriptional regulatory element database, new entries and other development. Nucleic Acids Res. 2007; 35:D137–140. Database issue. [PubMed: 17202159]

57. Awasthi A, Carrier Y, Peron JP, Bettelli E, Kamanaka M, Flavell RA, et al. A dominant function for interleukin 27 in generating interleukin 10-producing anti-inflammatory T cells. Nat Immunol. 2007; 8(12):1380–1389. [PubMed: 17994022]

58. Xiao S, Jin H, Korn T, Liu SM, Oukka M, Lim B, et al. Retinoic acid increases Foxp3+ regulatory T cells and inhibits development of Th17 cells by enhancing TGF-beta-driven Smad3 signaling and inhibiting IL-6 and IL-23 receptor expression. J Immunol. 2008; 181(4):2277–2284. [PubMed: 18684916]

59. Amit I, Garber M, Chevrier N, Leite AP, Donner Y, Eisenhaure T, et al. Unbiased reconstruction of a mammalian transcriptional network mediating pathogen responses. Science. 2009; 326(5950):257–263. [PubMed: 19729616]

60. Jux B, Kadow S, Esser C. Langerhans cell maturation and contact hypersensitivity are impaired in aryl hydrocarbon receptor-null mice. J Immunol. 2009; 182(11):6709–6717. [PubMed: 19454665]

61. Durant L, Watford WT, Ramos HL, Laurence A, Vahedi G, Wei L, et al. Diverse targets of the transcription factor STAT3 contribute to T cell pathogenicity and homeostasis. Immunity. 2010; 32(5):605–615. [PubMed: 20493732]

62. Yang XP, Ghoreschi K, Steward-Tharp SM, Rodriguez-Canales J, Zhu J, Grainger JR, et al. Opposing regulation of the locus encoding IL-17 through direct, reciprocal actions of STAT3 and STAT5. Nat Immunol. 2011; 12(3):247–254. [PubMed: 21278738]

63. Shi LZ, Wang R, Huang G, Vogel P, Neale G, Green DR, et al. HIF1alpha-dependent glycolytic pathway orchestrates a metabolic checkpoint for the differentiation of TH17 and Treg cells. J Exp Med. 2011; 208(7):1367–1376. [PubMed: 21708926]

64. Yosef N, Shalek AK, Gaublomme JT, Jin H, Lee Y, Awasthi A, et al. Dynamic regulatory network controlling TH17 cell differentiation. Nature. 2013; 496(7446):461–468. [PubMed: 23467089]
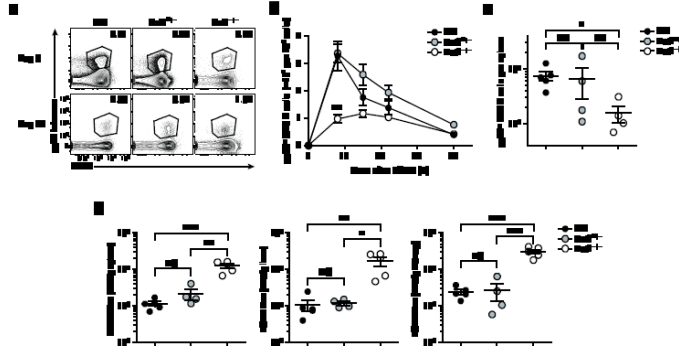
Figure 1. BATF is required for effector CD8+ T cell differentiation and viral control

Batf^{−/−}, *Batf*^{+/−}, and wild-type mice (C57Bl/6 background) were intraperitoneally infected with LCMV Arm (2×10^5 pfu) and analyzed at the indicated time points. (**a**) Flow cytometry plots gated on CD8+ cells showing percentage of gp33-specific cells at d8 and d40 p.i. in the blood. (**b**) Number of gp33-specific CD8+ T cells per 1×10^6 cells in the blood. Mean±s.e.m. (**c**) Number of gp33-specific CD8+ T cells at d8 p.i. in the spleen. Mean±s.e.m. (**d**) Viral titers in the spleen, liver and kidney at d5 p.i. Mean ±sem. Data are representative of two independent experiments (n=3-5 per time-point). Each symbol (**b** and **d**) represents an individual mouse. *P<0.05, **P<0.01, ***P<0.001 (unpaired Student's *t*-test).
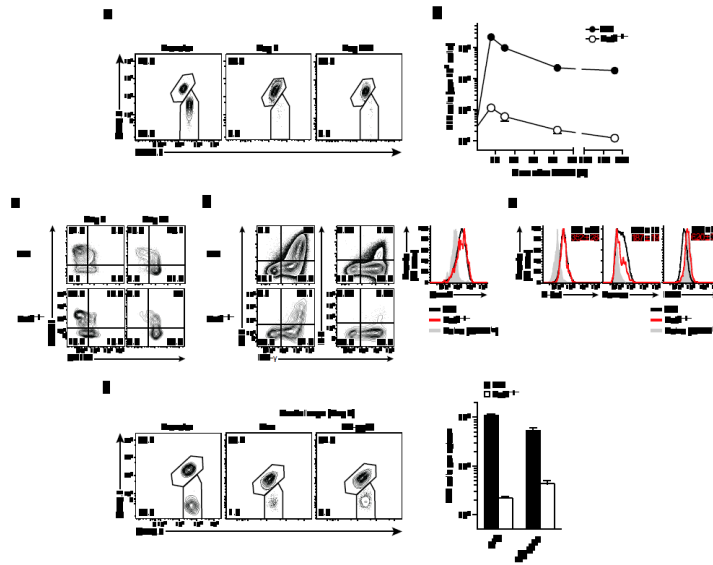
Figure 2. BATF acts cell-intrinsically to regulate CD8$^+$ T cell effector differentiation

Congenically different *Batf*$^{-/-}$ and wild-type P14 cells (total $5\times10^2 \sim 1\times10^4$ cells) were mixed at 1:1 ratio and adoptively transferred to naive recipients. The recipient mice were intraperitoneally infected with LCMV Arm (2×10^5 pfu) and analyzed at indicated time-points. (**a**) Flow cytometry plots gated on P14 cells showing percentage of wild-type (upper, CD45.1$^+$CD45.2$^+$) and *Batf*$^{-/-}$ (lower, CD45.1$^+$) at adoptive transfer and d7 and d224 in the spleen. (**b**) Number of *Batf*$^{-/-}$ and wild-type P14 cells per 1×10^6 cells in the blood. (**c** - **e**) Plots gated on wild-type or *Batf*$^{-/-}$ P14 cells showing CD127 and KLRG1 expression at d8 and d44 (**c**), and cytokine production and granzyme B expression at d8 (**b**), and expression level of transcription factors at d8 (**e**). (**e**) Numbers in the plots indicate MFI (mean±2s.d.). (**f**) Requirement of BATF for secondary response. Wild-type (CD45.1$^+$CD45.2$^+$) and *Batf*$^{-/-}$ (CD45.2$^+$) memory P14 cells were generated in separate hosts (CD45.1$^+$) and isolated from spleen at d51 after primary infection. Equal numbers of wild type and *Batf*$^{-/-}$ memory P14 cells were mixed (total 7×10^3 cells) and adoptively transferred into secondary hosts (CD45.1$^+$). One day later recipient mice were infected with LCMV Arm (2×10^5 pfu) or LM-gp33 (1×10^4 cfu), and analyzed at d7 p.i. Data are representative of three (**a-e**) and two (**f**) independent experiments (n=3-5 per time point).
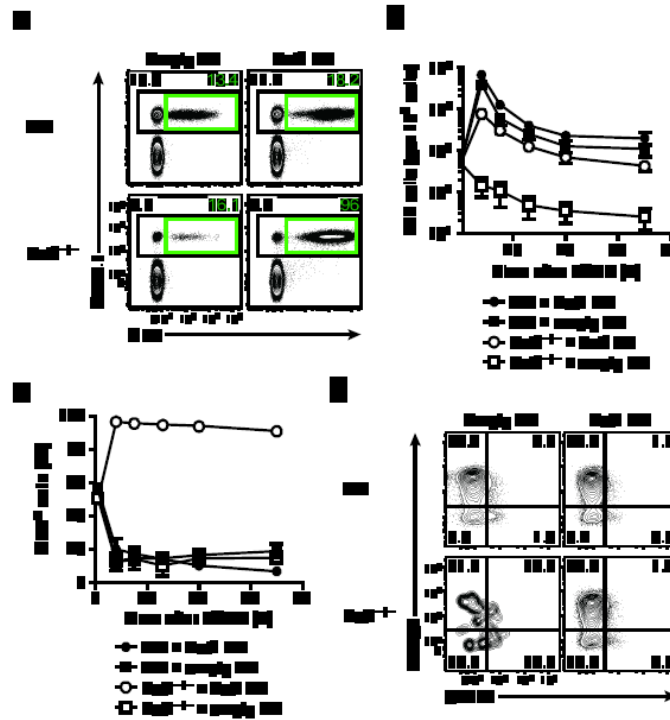
Figure 3. BATF overexpression rescues effector differentiation in *Batf*^{−/−} effector CD8⁺ T cells

CD45.1$^+$ *Batf*$^{-/-}$ and wild-type P14 cells were transduced with *Batf* overexpressing retrovirus (*Batf* RV) or empty retrovirus (Empty RV) one day after stimulation with anti-CD3 and anti-CD28 antibodies *in vitro*. Transduced P14 cells (1×10^4 cells) were transferred into time-matched CD45.2$^+$ mice (one day after LCMV Arm infection). (**a**) Plots gated on CD8$^+$ cells show the frequency of GFP$^+$ P14 cells at d8 p.i. in the blood. Numbers in the plots indicate percent of P14 cells among total CD8$^+$ T cells (upper left, black gate) and percent of GFP$^+$ cells among total P14 cells (upper right, green gate). (**b**) Number of P14 cells per 1×10^6 cells in the blood. Mean±s.e.m. (**c**) Frequency of GFP$^+$ cells among the transferred P14 cells in (**b**), tracked longitudinally in peripheral blood from mice infected with Arm. Mean±s.e.m. (**d**) Expression of CD127 and KLRG1 on GFP$^+$ donor P14 cells at d8 p.i. Numbers in the plots indicate percent of each quadrant gate. Data are from four independent experiments (n=4-5 per time point).
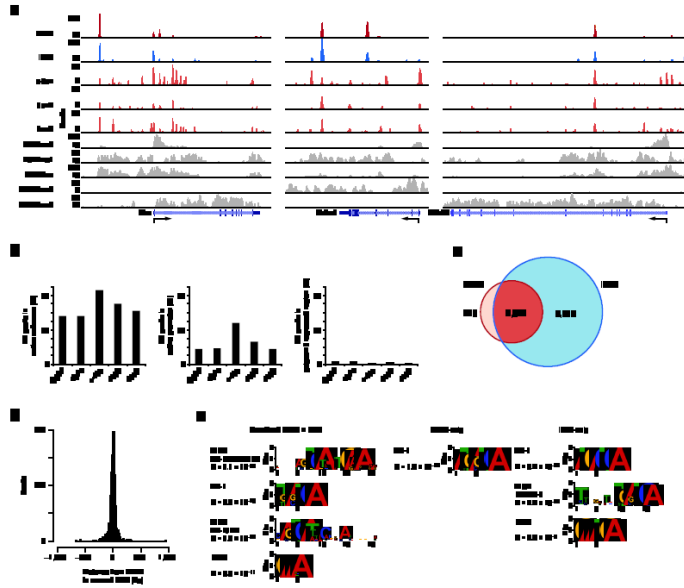
Figure 4. BATF and IRF4 co-bind in effector CD8^{+} T cells

ChIP-Seq analysis of wild-type effector CD8^{+} T cells. (**a**) ChIP-Seq binding tracks for BATF (Red), IRF4 (Blue), Jun transcription factors (orange), and modified histones (gray) at representative genes (*Il2ra*, *Prdm1, Il12rb2*). (**b**) Bar graphs indicating the percentage of TF peaks within active enhancers (left), active promoters (middle), and Polycomb repressed (right) chromatin states for each TF. (**c**) Venn diagram of the number of genes bound by BATF and IRF4. *P*<2×10^{−16}. Significance was assessed with a binomial probability test. (**d**) Distribution analysis of the combined BATF and IRF4 regions. The histogram shows the distribution of midpoint distances between a BATF site and the nearest IRF4 site in a 1 kb window. (**e**) *De novo* motif analysis of the combined BATF and IRF4 regions, BATF-only regions, and IRF4-only regions.
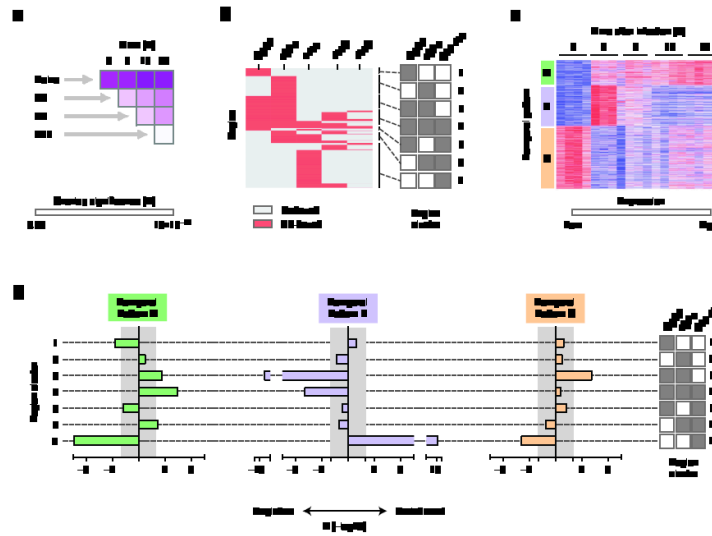
Figure 5. Temporal regulation of gene expression during effector CD8^{+} T cell differentiation by combinatorial binding of BATF, IRF4 and Jun

(**a**) Overlap of BATF target genes with genes up- or down-regulated during effector CD8^{+} T cell differentiation (FDR < 0.25 and fold change > 2 or < −2). Significance between each pair-wise combination tested with a hypergeometric test, and 1-(Log$_{10}$)P value indicated by color scale. (**b**) Clustered heat-map of regions bound by combinations of TFs (red, bound; grey, unbound), and the seven resulting combinations of TF binding indicated by the legend on the right. (**c**) k-means clustering of gene expression in P14 CD8^{+} T cells following LCMV Arm infection measured at indicated time-points. (**d**) Overlap between clusters of genes bound by combinations of TFs from (**b**) and temporal patterns of gene expression from (**c**). Each bar denotes whether a TF region cluster exhibits significant depletion (negative values) or enrichment (positive values) within the genes of the indicated temporal pattern. Significance, measured by the hypergeometric test, for each TF cluster genes in Pattern A (left), Pattern B (middle), and Pattern C (right).
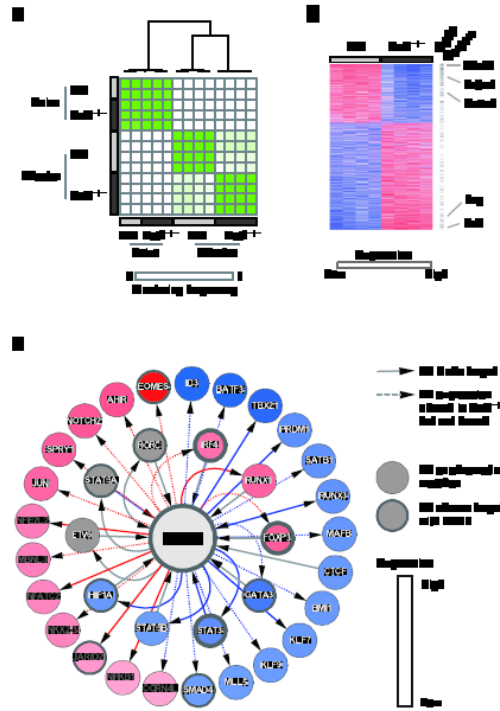
Figure 6. Loss of BATF perturbs a network of transcription factors
(**a**) Consensus clustering of gene expression in naive and *in vitro* generated effector CD8^{+} T cells using wild-type or *Batf*^{−/−} CD8^{+} T cells. (**b**) Heatmap of genes differentially expressed (FDR < 0.25) in wild-type and *Batf*^{−/−} CD8^{+} T cells. BATF target genes are marked by the grey bars to the right of the heatmap. (**c**) BATF-centric interaction network of TFs. Incoming or outgoing connections are indicated by arrow direction; differential expression of TFs in *Batf*^{−/−} effector CD8 T cells is indicated by color of node and edge (Red for increased expression in *Batf*^{−/−} cells and Blue for decreased expression in *Batf*^{−/−} cells); and presence of shared target genes indicated by thick node outline.
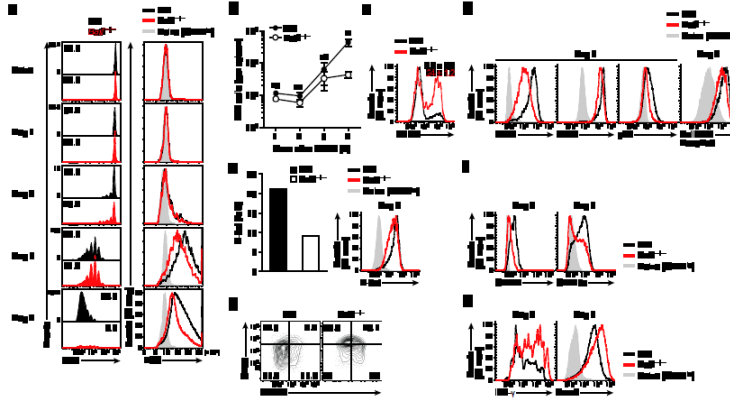
Figure 7. Loss of BATF perturbs the earliest stages of effector CD8$^+$ T cell differentiation

Batf$^{-/-}$ (CD45.2$^+$) and wild-type (CD45.1$^+$CD45.2$^+$) P14 cells were mixed at a 1:1 ratio and transferred to CD45.1$^+$ mice (total 1~2×10^6 cells) after labeling with CFSE or Cell Trace Violet (CTV). The recipient mice were infected with LCMV Arm (2×10^5 pfu). (**a**) Proliferation was assessed by CTV dilution and longitudinal cell size (FSC) of *Batf*$^{-/-}$ and wild-type P14 cells was examined. Y-axis in CTV histogram was adjusted to the same scale to reflect relative number of both P14 cell types at a given time point. Numbers in the plots indicate percent of *Batf*$^{-/-}$ and wild-type cells among total P14 cells. (**b**) Number of P14 cells per spleen. Mean±s.e.m. *p=0.0212 (unpaired Student's *t*-test). (**c**) Measurement of caspase activity by FLICA staining at d3. Numbers in the histogram indicate percent FLICA positive. Mean±s.e.m. (**d**) Expression of nutrient transporters, phosphorylation of the S6 ribosomal protein and reactive oxygen species production. (**e**) Fold increase of T-bet expression in *Batf*$^{-/-}$ and wild-type P14 cells at 4 hrs after *in vitro* anti-CD3 and anti-CD28 stimulation, determined by Affymetrix chip (left), and T-bet protein level at d3 *in vivo* (right). (**f-h**) Expression of cytokine receptors (**f**), CD62L and CD69 at d3 (**g**), and IFN-γ production upon *in vitro* restimulation (d2) and granzyme B expression *ex vivo* (d3) (**h**). Time points for analysis are shown in histogram (**d**, **e**, **f** and **h**). Data are representative of four independent experiments (n=3-5 per time point).

Table 1

BATF target genes.

Transcription Factor	T Cell Activation	Cytokine Signaling	Effector Function	Homing	Apoptosis	Metabolism
Tbx21	*Cd28*	*Il12rb2*	*Gzmb*	*Cd44*	*Bcl2l1*	*Gpi1*
Eomes	*Ctla4*	*Il18rap*	*Ifng*	*Cxcr3*	*Casp3*	*Hk2*
Prdm1	*Lag3*	*Il2ra*	*Il18*	*Ccr1*	*Bcl2*	*Acly*
Rora	*Cd86*	*Il2rb*	*Ccl3*	*Ccr2*	*Mcl1*	*Cs*
Runx1	*Tnfrsf8*	*Il10*	*Ccl5*	*Adam17*	*Fas*	*Dlst*
Runx2	*Tnfrsf9*	*Casp1*	*Ifna2*	*Adam19*	*BCl2l11*	*Suclg2*
Hif1a	*Cd274*	*Il6st*	*Ifnab*	*Sell*	*Bmf*	*Rptor*
Fosl2	*Havcr2*	*Ifngr2*	*Il2*	*Sele*		*Gsk3a*
Atf3	*Cd3d*	*Tgfbr2*		*Ccr7*		*Rpl13*
Atf4	*Cd3g*	*Il21r*		*Ccr9*		*Rps6ka1*
Tcf7	*Cd247*	*Ifnar2*		*Ccl20*		*Ogdh*
Bcl6	*Cd276*	*Tgfbr3*		*Selp*		*Phkb*
Lef1	*Cd27*	*Il12rb1*		*Ccr4*		*Rpl23a*
Ikzf2	*Btla*	*Ifnar1*		*Ccr6*		*Rps3*
Stat3	*Tnfrsf4*	*Il21*		*Cxcr6*		*Rpl24*
Stat4	*Csk*	*Il23r*		*Adam22*		*Rps9*
Stat5b		*Il1r1*				*Rpl35*
Ikzf1		*Il1r2*				*Rps19*